

# Water Transport in Crosslinked 2-Hydroxyethyl Methacrylate

K. F. CHOU,<sup>(1)</sup> C. C. HAN,<sup>(2)</sup> and SANBOH LEE<sup>(1)</sup>

<sup>(1)</sup>*Department of Materials Science  
National Tsing Hua University  
Hsinchu, Taiwan*

<sup>(2)</sup>*Polymers Division  
National Institute of Standards and Technology  
Gaithersburg, Maryland 20899*

Water transport in crosslinked 2-hydroxyethyl methacrylate (HEMA) was investigated. Crosslinked HEMA was irradiated by gamma ray in vacuum for this study. The sorption data of de-ionized water transport in crosslinked HEMA subjected to various gamma ray dosages are in excellent agreement with Harmon's model which accounts for Case I, Case II, as well as the anomalous transport processes. The diffusion coefficient for Case I transport and velocity for Case II transport satisfy the Arrhenius equation for all dosages. The transport process was exothermic and the equilibrium-swelling ratio satisfied the van't Hoff plot. The pH value of de-ionized water after the sorption/de-sorption treatment of the irradiated crosslinked HEMA specimen was analyzed. The transmittance of irradiated crosslinked HEMA treated by de-ionized water was also studied. The effect of irradiation on the polymer chains was revealed by the measurement of glass transition temperature and the quantitative determination of water structures in crosslinked HEMA hydrogel. The UV cut-off wavelength of crosslinked HEMA shifted to longer wavelength side with increasing irradiation dosage, but the trend of transmittance after water treatment was opposite. The effect of specimen thickness on water transport was also studied.

## 1. INTRODUCTION

Hydrophilic polymers based on 2-hydroxyethyl methacrylate (HEMA) have been widely studied because of their high water content, non-toxicity and favorable tissue compatibility, which leads to many applications as bio-compatible-materials. These applications include soft contact lenses (1, 2), kidney dialysis systems (3, 4), drug delivery systems (5, 6), and artificial liver support systems (7, 8). The presence of a hydroxyl group and a carbonyl group on each repeat unit makes this polymer compatible with water, and the hydrophobic  $\alpha$ -methyl group and backbone impart hydrolytic stability to the polymer and support the mechanical strength of the polymer matrix (9–11). Several research groups (12–16) have investigated different states and properties of water molecules within the crosslinked HEMA gels and also the equilibrium-swelling behavior of HEMA with water. However, they have concentrated on the study of the equilibrium state instead of the kinetics of transport of solvent in the crosslinked HEMA despite the fact that several kinetics models have been proposed. Yasuda *et al.* (17) proposed that the relationship between the diffusive

permeability of water and the hydraulic permeability of water is a function of the volume fraction of water in swollen polymer membranes. Peppas *et al.* (18) suggested that the mechanism of release diffusive solute may be obtained through the swelling interface number, which is defined as the product of the maximum thickness of swollen phase and average penetration velocity divided by the diffusion coefficient of the solvent. Also, the influence of crosslinked HEMA composition on non-Fickian water transport through glassy copolymers has been investigated by Franson *et al.* (19).

Solvent transport process in glassy polymers has been categorized by Alfrey *et al.* (20) to include Case I (Fickian) transport, anomalous transport and Case II (stress relaxation) transport. In the Case I mechanism, mass flows from high concentration to low concentration through a random diffusion process, which has been studied by many researchers. For example, Crank (21) has collected many solutions of Case I with different initial and boundary conditions. In the Case II process, transport occurs when the mass moves with constant velocity controlled by swelling. The effect of swelling is correlated with the size of penetrant mole-

cules. Thomas and Windle (22), Hui *et al.* (23) and Govindjee and Simo (24) have investigated the theory of the Case II process. Additionally, a dual mode sorption model has been reported by Vieth *et al.* (25), which postulates the existence of two concurrent populations. One population is held by normal dissolution with Henry's law solubility constant and the other population sorbed into micro-voids throughout the polymer follows the Langmuir isotherm. This dual sorption model can be considered as a special kind of Case I transport process. Okamoto *et al.* (26) and Toi *et al.* (27) analyzed water vapor and gas transport in polyimide film using this dual sorption model. These studies did not report the anomalous transport behavior, which is a mixture of Case I and Case II transport processes. In general, the amount of penetrant absorbed per unit area is proportional to  $t^m$  where  $t$  is time and  $m=0.5$  for Case I,  $m=1$  for Case II and  $m=0.5\sim 1$  for anomalous transport. Kwei and co-workers (28–32) proposed a model that combines the Case I and Case II processes to explain the anomalous transport phenomena in semi-infinite medium. Harmon *et al.* (33, 34) modified the equation proposed by Kwei *et al.* (28–32) to include the finite size. The results have been used in the analysis of the transport process of many organic solvent/polymer systems of finite size (35–38). This has prompted us to analyze water transport in crosslinked HEMA with this model. The purpose of studying the transport mechanism of the solvent/HEMA system is to find the best conditions to regulate the rate of drug release and to control the diffusion of water or tissue metabolites through crosslinked HEMA membranes.

One of the important factors controlling the swelling behavior of crosslinked HEMA is the balance of hydrophobic and hydrophilic interactions between polymer chains and water molecules. Refojo and Yasuda (39) found that the enthalpy of dilution,  $\Delta H_{dil}$ , was negative below  $T = 55^\circ\text{C}$  and positive above  $55^\circ\text{C}$ , which resulted from the competition of the water-water dispersion forces and the water-polymer interaction forces. The balance of hydrophobic and hydrophilic forces in a polymer could be controlled by the addition of crosslinking agent and by varying the hydrophobic co-monomer composition (13, 40–43). These processes could also be helpful in raising the selectivity of water content and mechanical strength of hydro-gel for different applications. In addition, the hydrophobic and hydrophilic interactions of polymer chains can be modified by the gamma ray irradiation, which induces crosslinking as well as chain scission. This is the motivation for us to study the effect of gamma ray irradiation on the thermal properties of crosslinked HEMA and water in hydro-gels.

## 2. EXPERIMENTAL PROCEDURE

Crosslinked HEMA was obtained from Canadian Contact Lens Laboratories Ltd., Montreal, Quebec, Canada, as soft contact lens blanks. They are of stand-

ard size, 12.8 mm diameter and 6.0 mm thickness. These blanks were mounted on a bench lathe and thinned to about 1.5 mm, and then ground on 600 and 1200 grit emery papers and polished with 1.0 and 0.05  $\mu\text{m}$  aluminum slurries. The final thickness of the specimen is 1.4 mm. An additional four sets of blanks were treated with the same grinding and polishing processes to a final thickness of 0.95, 1.2, 1.5, 1.8 mm, respectively. They were prepared for the study of the thickness effect on the water transport kinetics. Each specimen was annealed for one week in a vacuum chamber at  $60^\circ\text{C}$  (13) and furnace cooled to  $25^\circ\text{C}$ . The purpose of annealing is to reduce the residual stresses in crosslinked HEMA.

In addition to the standard specimens (non-irradiated), specimens were exposed to a 30000Ci Cobalt-60 source with a dosage rate of 7.1 kGy/h at the Isotope Center, the National Tsing Hua University, in vacuum and at room temperature. Specimens were exposed for different times to reach dosages of 160, 227, 397, 468 and 546 kGy, respectively. Before gamma ray irradiation, specimens were sealed in evacuated glass ampoules.

For the absorption study each specimen was pre-weighed. Then the specimens were preheated to the elevated temperature for water transport measurement and moved to a de-ionized water-filled glass bottle at the same temperature. The temperature was maintained by a thermo-statted water bath. The specimen was taken out periodically for measurement. The surfaces were blotted and then weighed with an Ohaus Analytical Plus digital balance. After weighing, the specimen was immediately returned to the water bath for the next measurement. The pH measurement of the solvent was conducted using a Jenco Electronics digital pH meter at  $25^\circ\text{C}$  after the absorption experiment.

For transmittance measurement, specimens with various  $\gamma$ -ray dosages were immersed in deionized water at different temperatures until saturation. Then each specimen was dehydrated in air at  $25^\circ\text{C}$ , and transmittance was measured in air using a Hitachi U-3210/U-3240 Spectrometer in the range of wavelength from 240nm to 800 nm.

For DSC study, specimens irradiated by  $\gamma$ -ray were cut into small pieces of 2.5–3.5 mg. Each specimen was either immersed in de-ionized water at  $40^\circ\text{C}$  until saturation before measurement or measured without water treatment. Each specimen was enclosed in an aluminum pan and inserted into a Seiko SSC II-5200H differential scanning calorimeter (DSC) for measurement. An inlet nitrogen flow of 40 ml/min was used during the measurement. The temperature was increased from  $25^\circ\text{C}$  to  $100^\circ\text{C}$  with a heating rate of  $5^\circ\text{C}/\text{min}$ . For the study of water structure, specimens immersed in water for different periods at  $35\text{--}55^\circ\text{C}$  were cooled from  $25^\circ\text{C}$  to  $-40^\circ\text{C}$  at a cooling rate of  $5^\circ\text{C}/\text{min}$ , and held at  $-40^\circ\text{C}$  for 20 min. Then they were heated from  $-40^\circ\text{C}$  to  $30^\circ\text{C}$  with heating rate of  $5^\circ\text{C}/\text{min}$ . The heat flow of the system was recorded.

### 3. RESULTS

#### 3.1 Water Transport: Effect of $\gamma$ -Ray

Harmon *et al.* (33) proposed a model that accounts for Case I, Case II and anomalous transport processes. In this model, a slab of polymer located between  $(-\ell, \ell)$  on the x-axis is surrounded with solvent. The dimensions of the slab in the other two directions (y and z) are assumed to be much larger than the thickness (x-direction); therefore, a one-dimensional model can be considered. The total flux,  $J$ , is assumed to consist of two components: one is due to the diffusion with a concentration gradient and the other is due to the stress relaxation of polymer chains with a propagation speed,  $v$ . Therefore,

$$J = -D \frac{\partial C}{\partial X} + v(C - C_{0x}) \text{ for } 0 \leq X \leq \ell \quad (1)$$

where  $C$  and  $C_{0x}$  are concentrations at points  $X$  and  $X = 0$ , respectively. The diffusivity  $D$  and velocity  $v$  comes from the Case I and Case II transport processes. The diffusivity is always larger than or equal to zero, but the velocity can be negative (or positive) if the direction of Case II transport is from the outer surface to the center (or vice versa). Because of geometric symmetry, Eq 1 is also valid in the region  $-\ell \leq X \leq 0$  if the sign of velocity is changed. Equation 1 ensures that the flux is always zero at the center because of this geometric symmetry. According to the mass conservation, one can also write the following equation,

$$\frac{\partial C}{\partial t} = D \frac{\partial^2 C}{\partial X^2} - v \frac{\partial C}{\partial X} \text{ for } 0 \leq X \leq \ell \quad (2)$$

The solvent concentration at the surfaces,  $x = \pm \ell$ , can be assumed as a constant value,  $C_0$ , at all times ( $t > 0$ ) and the slab is solvent-free at the initial time. Equation 2 with the boundary condition of constant surface concentration,  $C_0$ , at  $x = \pm \ell$  can be solved using the Laplace transformation. After integrating the concentration in the slab, Harmon *et al.* (33) obtained the weight gain  $M_t$  at time  $t$  as

$$\frac{M_t}{M_\infty} = 1 - 2 \sum_{n=1}^{\infty} \frac{\lambda_n^2 \left( 1 - 2 \cos \lambda_n \exp \left( -\frac{v\ell}{2D} \right) \right)}{\beta_n^4 \left( 1 - \frac{2D}{v\ell} \cos^2 \lambda_n \right)} \exp \left( -\frac{\beta_n^2 Dt}{\ell^2} \right) \quad (3)$$

where

$$\lambda_n = \frac{v\ell}{2D} \tan \lambda_n \quad (4)$$

$$\beta_n^2 = \frac{v^2 \ell^2}{4D^2} + \lambda_n^2 \quad (5)$$

The roots of Eq 4 ( $\lambda_n$  with  $n=1,2,3,\dots,\infty$ ) were used in Eq 3 and Eq 5 and  $M_\infty$  is the final equilibrium weight of solvent in the specimen.

Two limiting cases are worthwhile to mention. First, when  $v$  is equal to zero, Eqs 4 and 5 become  $\lambda_n = (n + 1/2)\pi$  and  $\beta_n = \lambda_n$ , respectively. Therefore, Eq 3 is reduced to

$$\frac{M_t}{M_\infty} = 1 - \frac{8}{\pi^2} \sum_{n=0}^{\infty} \frac{1}{(2n+1)^2} \exp \left[ -(2n+1)^2 \pi^2 Dt/4\ell^2 \right] \quad (6)$$

This equation (Eq 6) is the same as that derived by Crank (21) for a simple diffusion case. Second, when  $D$  is equal to zero, weight gain can be directly obtained from Eq 2 as

$$\frac{M_t}{M_\infty} = \frac{|v|t}{\ell} \quad (7)$$

where  $t$  is less than  $\ell/|v|$ .

The data for de-ionized water transport in irradiated and crosslinked HEMA at temperatures from 35 to 55°C are shown in Fig. 1(a)-(e) where  $M_0$  ( $=0.2018 \pm 0.0050$  g) is the initial weight of specimen. Note that the shape of crosslinked HEMA for dosage 546 kGy after immersion in water becomes irregular so that the sorption study was not carried out. These data can be analyzed using the above model. The solid lines in Fig. 1 are plotted using Eq 3. It is found that the theoretical model is in excellent agreement with the experimental data. The values of  $D$  and  $v$  obtained from Fig. 1 are listed in Table 1. Both  $D$  and  $v$  increase with the increase of temperature for a given dosage ( $\phi$ ) and decrease with the increase of dosage for a given temperature. Water transport based on both Case I and Case II mechanisms move from the outer surface to the center. Both  $D$  and  $v$  satisfy the Arrhenius equation; their activation energies are calculated and tabulated in Table 2. The activation energy of  $v$  decreases monotonically with increasing dosage, but that of  $D$  is independent of dosage.

The equilibrium-swelling ratio of water,  $S$ , is determined by the ratio of the saturated weight gain to the weight of dry polymer. The data of  $S$  at different temperatures with various dosages are listed in Table 1. For a given dosage, the value of  $S$  decreases with increasing temperature. That is, the mass transport is an exothermic process. The equilibrium-swelling ratio can be curve-fitted to a van't Hoff plot, and the heat of mixing  $\Delta H$  for different dosages are listed in Table 2. The heat of mixing is greater for the standard specimens than for the specimens with dosage  $\phi \cong 160$  kGy. It is also found that the heat of mixing is nearly same for the dosage in the range of 160 and 468 kGy. For a given temperature, the value of  $S$  decreased with increasing dosage.

#### 3.2 pH Value

The pH values of the solvent after the mass transport experiment at different temperatures for various dosages are tabulated in Table 3. The pH value of de-ionized water at 25°C is 6.1. For a standard specimen,

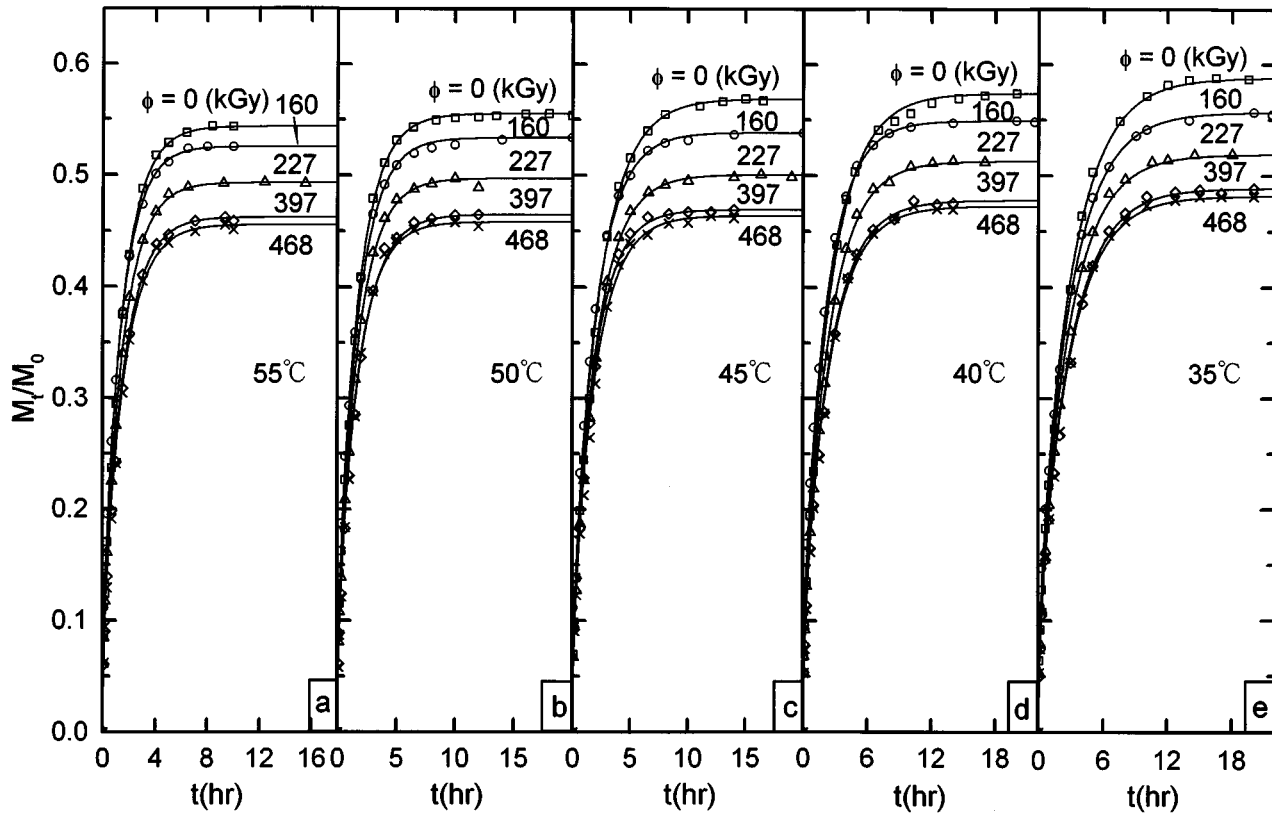


Fig. 1. Water sorption in crosslinked HEMA irradiated by  $\gamma$ -ray in vacuum: (a)  $T = 55^\circ\text{C}$ , (b)  $T = 50^\circ\text{C}$ , (c)  $T = 45^\circ\text{C}$ , (d)  $T = 40^\circ\text{C}$  and (e)  $T = 35^\circ\text{C}$ .

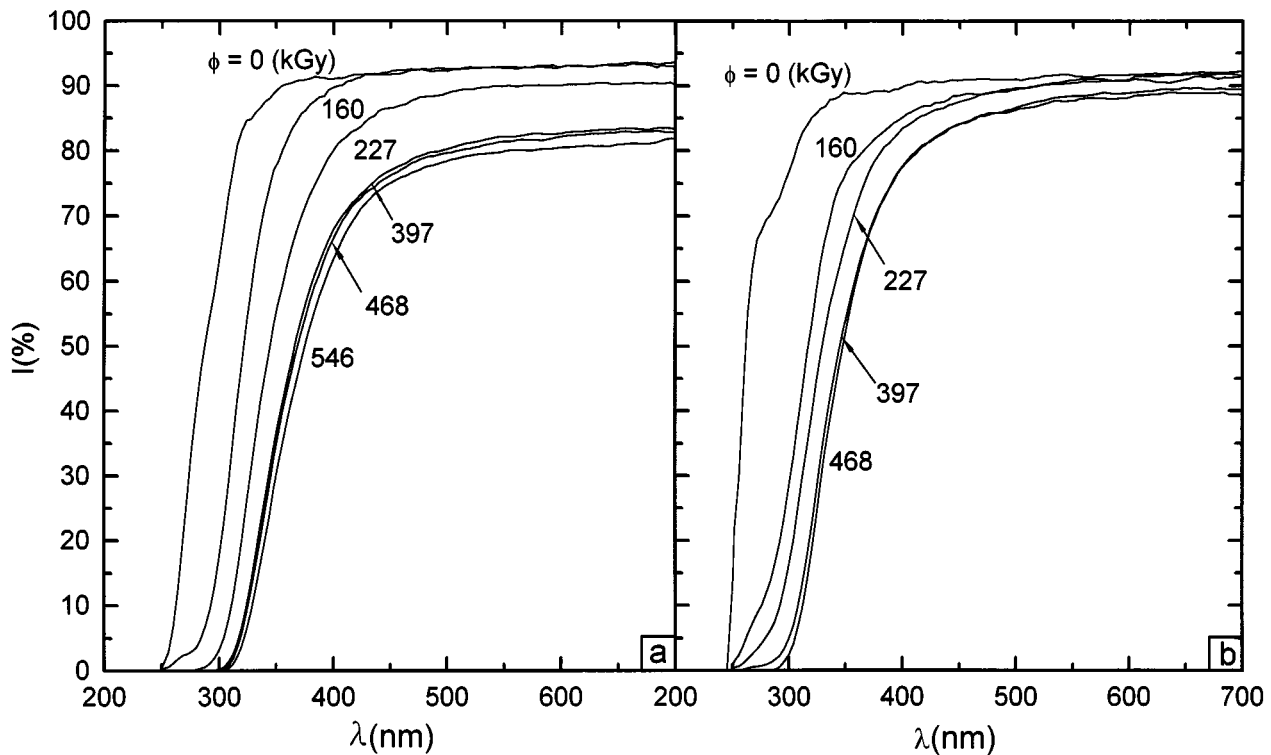


Fig. 2. Transmission spectrum of standard specimen and irradiated crosslinked HEMA: (a) before water absorption and (b) after water saturation at  $55^\circ\text{C}$ .

**Table 1. The Diffusion Coefficient D for Case I, Velocity v for Case II and Equilibrium-Swelling Ratio S in Water / Crosslinked Irradiated HEMA (Irradiated in Vacuum).**

T (K)	$\phi$ (kGy)	$D \times 10^7$ (cm <sup>2</sup> /sec)	$v \times 10^6$ (cm/sec)	S (wt%)
328	0	3.10	2.90	54.35 ± 0.18
	160	3.00	2.80	52.53 ± 0.24
	227	2.90	2.70	49.31 ± 0.22
	397	2.80	2.60	46.23 ± 0.21
	468	2.75	2.55	45.56 ± 0.21
323	0	2.60	2.40	55.53 ± 0.25
	160	2.58	2.35	53.37 ± 0.24
	227	2.50	2.30	49.72 ± 0.22
	397	2.43	2.25	46.51 ± 0.21
	468	2.40	2.22	45.84 ± 0.21
318	0	2.20	2.00	56.88 ± 0.26
	160	2.15	1.95	53.84 ± 0.24
	227	2.10	1.95	50.07 ± 0.23
	397	2.05	2.02	46.94 ± 0.21
	468	2.10	2.00	46.40 ± 0.21
313	0	1.90	1.70	57.36 ± 0.26
	160	1.85	1.70	54.90 ± 0.25
	227	1.82	1.72	51.27 ± 0.23
	397	1.77	1.72	47.77 ± 0.22
	468	1.72	1.78	47.24 ± 0.21
308	0	1.60	1.40	58.77 ± 0.27
	160	1.57	1.40	55.67 ± 0.25
	227	1.52	1.45	51.90 ± 0.23
	397	1.47	1.48	48.89 ± 0.22
	468	1.46	1.56	48.20 ± 0.22

the acidic products from the water-induced hydrolysis of an ionizable group of the polymer dissolve back into the solvent, so that the pH value of the solvent after mass transport is lowered. The pH value decreases with increasing temperature. That is, the hydrolysis process is endothermic. For a standard specimen, the reaction heat is obtained from the slope of logarithmic hydrogen ion increment ( $\Delta[H^+]$ ) in the solvent versus the reciprocal of mass transport temperature. Note

that pH value is equal to the negative logarithmic hydrogen ion concentration. The hydrogen ion increment is determined by the ratio of the difference of  $H^+$  concentration after and before mass transport to the  $H^+$  concentration in the solvent before mass transport. The value of reaction heat obtained is 19.657 kcal/mole for the standard specimen. However, for the irradiated polymer, the  $\gamma$ -ray excites the ionizable group by creating free radicals on polymer chains. Acidic ions are produced by hydrolysis so that the pH value of solvent with irradiated specimen is lower than that with standard specimen. On the other hand, for a given irradiation dosage, the pH value does not simply increase with decreasing temperature; the trend is reversed at 45°C. Owing to the excitation of ionizable group, the enthalpy for hydrolysis is reduced. The thermal effect on the reaction for irradiated polymer is not so significant as that for a standard polymer. Moreover, the more water content in hydrogel at lower temperature supports the hydrolysis of ionizable groups. The thermal effect dominates at high temperatures, whereas the influence of water content is significant at low temperatures. Both mechanisms are favorable for acidifying the solvent. In order to prove that there are chain scissions and some acidic groups from the crosslinked HEMA dissolved in the de-ionized water, the weight loss of crosslinked HEMA after dehydration is shown in Table 4. It is found that the weight loss increases with increasing dosage at a given temperature. Although the weight loss is not monotonic with respect to the temperature, the trend of weight loss is opposite to that of pH value. That is, the greater the acidity, the greater the weight loss.

### 3.3 Transmittance in UV-Visible Spectrum

The transmittance,  $I$ , as a function of wavelength,  $\lambda$ , for various dosages before and after water uptake is plotted in Figs. 2a and 2b, respectively. In the range of the visible spectrum (400–800 nm), it is found that

**Table 2. Activation Energies of Case I ( $E_D$ ) and Case II ( $E_V$ ) Transport and the Heat of Mixing  $\Delta H$ .**

$\phi$ (kGy)	0	160	227	397	468
$E_D$ (kcal/mole)	6.84 ± 0.15	6.80 ± 0.13	6.73 ± 0.08	6.71 ± 0.09	6.69 ± 0.28
$E_V$ (kcal/mole)	7.53 ± 0.13	7.15 ± 0.18	6.41 ± 0.16	5.83 ± 0.19	5.03 ± 0.13
$\Delta H$ (kcal/mole)	0.788 ± 0.59	0.603 ± 0.030	0.556 ± 0.063	0.581 ± 0.077	0.598 ± 0.059

**Table 3. pH Value of the Solvent After Mass Transport at 25°C.**

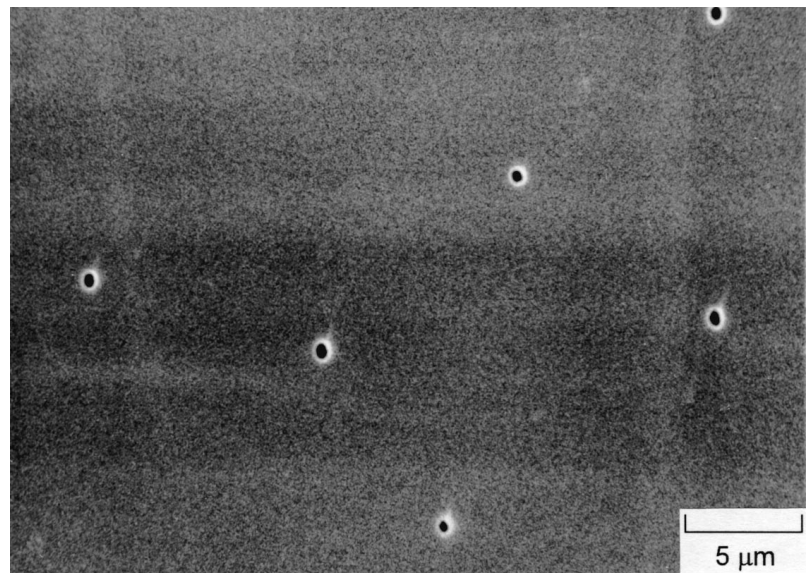
Mass Transport Temperature(K)	$\phi$ (kGy)				
	0	160	227	397	468
328	5.23 ± 0.01	4.77 ± 0.01	4.47 ± 0.01	4.25 ± 0.02	4.14 ± 0.02
323	5.41 ± 0.02	4.80 ± 0.02	4.51 ± 0.02	4.34 ± 0.03	4.25 ± 0.03
318	5.60 ± 0.01	4.99 ± 0.02	4.56 ± 0.02	4.40 ± 0.02	4.30 ± 0.02
313	5.71 ± 0.02	4.86 ± 0.01	4.56 ± 0.03	4.41 ± 0.01	4.26 ± 0.02
308	5.82 ± 0.01	4.72 ± 0.02	4.49 ± 0.02	4.38 ± 0.02	4.21 ± 0.03

**Table 4. The Weight Loss (wt%) of Crosslinked HEMA After Dehydration at Different Temperatures T for Various Dosages  $\phi$ .**

T(K)	$\phi$ (kGy)				
	0	160	227	397	468
328	0.072 $\pm$ 0.008	0.184 $\pm$ 0.007	0.272 $\pm$ 0.006	0.395 $\pm$ 0.008	0.481 $\pm$ 0.009
323	0.054 $\pm$ 0.008	0.181 $\pm$ 0.004	0.263 $\pm$ 0.008	0.373 $\pm$ 0.005	0.475 $\pm$ 0.006
318	0.049 $\pm$ 0.006	0.168 $\pm$ 0.006	0.252 $\pm$ 0.005	0.372 $\pm$ 0.007	0.466 $\pm$ 0.005
313	0.023 $\pm$ 0.003	0.175 $\pm$ 0.007	0.257 $\pm$ 0.004	0.363 $\pm$ 0.006	0.469 $\pm$ 0.007
308	0.013 $\pm$ 0.005	0.180 $\pm$ 0.004	0.265 $\pm$ 0.006	0.376 $\pm$ 0.007	0.471 $\pm$ 0.004

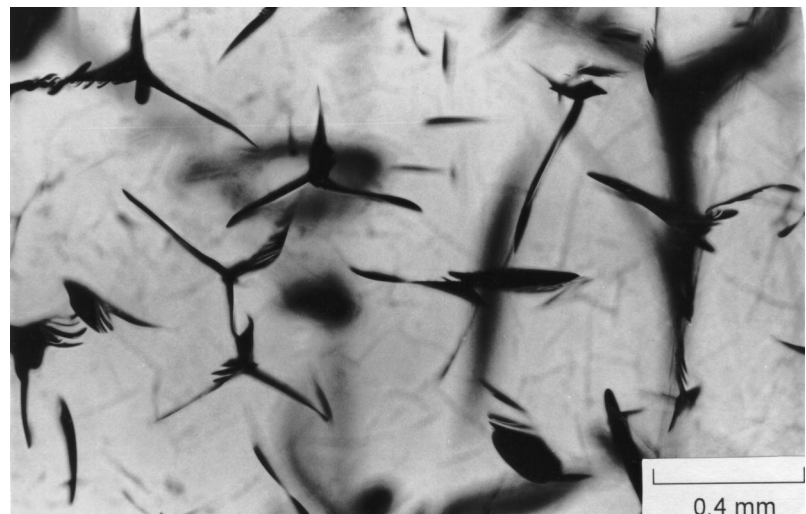
the transmittance for a standard specimen after water treatment is lower than that before water treatment. This is because water creates holes (or voids) in crosslinked HEMA when it penetrates the crosslinked polymer. After dehydration, holes may not be fully closed (see Fig. 3a), then light is scattered and transmittance is lowered for the standard specimens. For crosslinked

HEMA,  $\gamma$ -ray irradiation created color centers and/or cracks ( $\phi \geq 397$  kGy) in the specimen, so that the transmittance is reduced, as shown in Fig. 2a. Some cracks in the irradiated specimen are created as shown in Fig. 3b for dosages above 397 kGy. However, color centers may be annihilated by hydrolysis, whereas cracks may be healed by swelling of the polymer.



(a)

Fig. 3. (a) A cross section of standard crosslinked HEMA saturated with water after desorption is observed by SEM. (b) A cross section of irradiated crosslinked HEMA (468 kGy) is observed by a optical microscope with transmission light.



(b)

These processes of elimination of defects generated by irradiation in the optical path are more pronounced than that of creation of holes after dehydration. Therefore, the transmittance of irradiated crosslinked HEMA after desorption is greater than that before absorption, as shown in *Fig. 2b*. In the range of the near UV (240–400 nm) spectrum, it is also found that light with wavelengths, below 250 nm was absorbed completely in standard specimens, but the cutoff wavelength ( $\lambda_c$ ) shifts to the short wavelength side after specimens were treated with water. This is the result of dissolution of chromophores (such as carbonyl group) or auxochromes (such as hydroxyl group) of polymers into water. On the other hand, the cutoff wavelength of the polymer after irradiation increases with increasing dosage (or right shift). It is caused by the introduction of unstable factors (such as free radicals) (44), which absorb the energy of light (45). After water treatment, some unstable factors disappear or are extracted by hydration, so that the cutoff wavelength shifts backward. From *Fig. 2a*, the cutoff wavelengths are 250, 253, 280, 298, 302 and 306 nm for the specimen with  $\phi = 0, 160, 227, 397, 468,$  and 546 kGy before water treatment, respectively. Similarly, the cutoff wavelengths are 240, 245, 248, 258 and 288 nm for the specimen with  $\phi = 0, 160, 227, 397$  and 468 kGy after water treatment. It is found that the cutoff wavelength is independent of water-treated temperature in the range of 35–55°C.

### 3.4 Thermal Analysis

The glass transition temperatures of irradiated crosslinked HEMA before immersion ( $T_{g1}$ ) and after saturated with water ( $T_{g2}$ ) listed in *Table 5*. Below 397 kGy, the change of  $T_{g1}$  is very small, but above 397 kGy,  $T_{g1}$  is reduced significantly. This means that either chain scission and crosslinking rates are equal or neither chain scission nor crosslinking arises from irradiation for low irradiation dosage, whereas more chain scission than crosslinking is induced by  $\gamma$ -ray for high dosage, so that  $T_{g1}$  is decreased. For a specimen after the water saturation procedure, besides  $\gamma$ -ray irradiation, the water immersion process could have altered the chemical structure or caused scission of the polymer chain, and the residual amount of water could also affect the glass transition temperature,  $T_{g2}$ , of this crosslinked HEMA. Even the equilibrium-swelling ratio in the specimens irradiated with 400 kGy is lowered;  $T_{g2}$  is also reduced by the scission of polymer chains.

Further investigation of the effect of irradiation on polymer chains is made by the DSC analysis of water

structures in hydrogels. The water structure in hydrogels generally is categorized into non-freezing (bound) and freezing (free) water (12, 43, 46–48). Non-freezing water means that water molecule is hydrogen bonded to the hydrophilic group of the polymer chain. As a result, the non-freezing water does not freeze at 0°C, and the content is related to the number of hydrophilic groups in the polymer. However, freezing water is, in a manner, pure water and independent of the polymeric environment. The freezing water content is affected by chain mobility or crosslink density in the polymer (13, 14, 40, 49). In the heating process of DSC analysis, freezing water presents an endothermic melting peak at 0°C, but non-freezing water does not. Thus, two types of water content in hydrogels can be determined by the DSC analysis (12–14, 49). The endothermic melting peaks of freezing water at 0°C for the saturated hydrogel are shown in *Fig. 4*. The area of peak produced by the melting of freezing water was calculated ( $\Delta H_{\text{freezing water}}$ ), and then the contents of freezing water and non-freezing water can be obtained by the following equation (49),

$$S_f = \frac{M_{\text{freezing water}}}{M_{\text{polymer}}} = \frac{\Delta H_{\text{freezing water}}}{\Delta h_{\text{em}} M_{\text{polymer}}} = S_t - S_{\text{nf}} \quad (8)$$

where  $S_f$ ,  $S_{\text{nf}}$  and  $S_t$  are the swelling ratios contributed by freezing water, non-freezing water and total water at time  $t$ , respectively.  $M$  represents the mass of sub-script component.  $\Delta h_{\text{em}}$  is the effective specific heat of fusion of the water contained in the polymer, which is different from the heat of fusion of pure water (49–51). Because the swelling ratio of non-freezing water ( $S_{\text{nf}}$ ) is constant for the specimen subjected to the same transport condition but with different total swelling ratio ( $S_t$ ),  $\Delta h_{\text{em}}$  can be obtained from the linear regression of *Eq 8*. Note that when time is infinity (or long enough), the swelling ratio becomes the equilibrium-swelling ratio. The data of DSC analysis are listed in *Table 6*. For a given dosage, the freezing water content follows the van't Hoff equation; heats of mixing for various dosages are tabulated in *Table 6*. It is found that the transport process is endothermic. The heat of mixing is almost independent of dosage in the range of  $\phi \leq 300$  kGy, but becomes lower at  $\phi = 400$  kGy. For a given temperature, the freezing water content in hydrogels decreases to a minimum and then increases rapidly with increasing dosage. The result implies that the crosslinks of polymer chains may be increased at low dosage of irradiation but not significantly; however, for a dosage above the critical value ( $> 300$  kGy), the scission of main chains is increased. Then the chain mobility is raised, and the freezing water con-

**Table 5. Glass Transition Temperature of Irradiated Crosslinked HEMA Before Mass Transport ( $T_{g1}$ ) and After Mass Transport ( $T_{g2}$ ) at 40°C.**

$\phi$ (kGy)	0	160	220	300	397	468	546
$T_{g1}$ (K)	327 ± 2	326 ± 3	328 ± 3	328 ± 3	326 ± 4	323 ± 3	321 ± 4
$T_{g2}$ (K)	289 ± 3	290 ± 2	293 ± 3	297 ± 3	290 ± 5	287 ± 4	283 ± 4

tent increases. This is in agreement with the observation in the previous sections. On the other hand, the non-freezing water content also follows the van't Hoff equation, with a transport process, which is exothermic. The heat of mixing is greater for the standard specimen than for the specimen with  $\phi \geq 160$  kGy, although the total equilibrium-swelling ratios are similar. The non-freezing water content decreases monotonically with increasing dosage. This reduction of non-freezing water content is due to the destruction of hydrophilic groups by  $\gamma$ -ray. The decreasing rate of hydrophilic groups with increasing dosage is probably caused by the more rapid chain scission and extraction.

### 3.5 Water Transport: Effect of Thickness

The de-ionized water transport in crosslinked HEMA of various thickness,  $L$ , is displayed in Figs. 5 a-e. The solid lines are calculated using Eq 3 to fit the experimental data. It is found that the theoretical model is in excellent agreement with the experimental results. The directions of water transport based on both Case I and Case II are from outer surface to the center of specimen. The values of  $D$  and  $v$  obtained from Fig. 5 are calculated and tabulated in Table 7. At a given temperature, both  $D$  and  $v$  increase with increasing thickness. For a given thickness,  $D$  and  $v$  satisfy the Arrhenius equation; their activation energies are

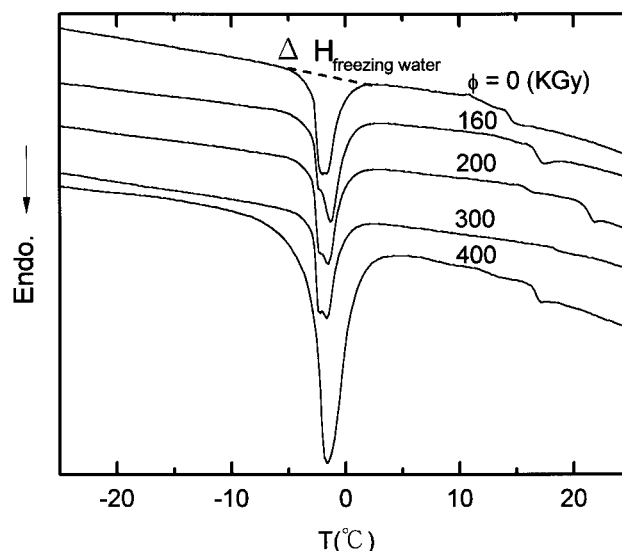


Fig. 4. DSC melt endothermic diagram of water in HEMA hydrogel for different dosages.

tabulated in Table 8. The activation energies for both Case I and Case II transport are almost the same regardless of thickness. Both aged (for 5 years) and fresh specimens are used for thickness and  $\gamma$ -ray studies. Compare Table 1 for  $L = 1.4$ mm (aged sample) and Table 7 for  $L = 1.5$ mm (fresh sample); the

Table 6. Total Equilibrium-Swelling Ratio ( $S_t$ ), Equilibrium-Swelling Ratios of Freezing Water ( $S_f$ ) and Non-Freezing water ( $S_{nf}$ ), Effective Specific Heat of Fusion of Water ( $\Delta h_{em}$ ) and Heats of Mixing of Non-Freezing Water ( $\Delta H_{nf}$ ) and Freezing Water ( $\Delta H_f$ ) in Hydrogel Based on Crosslinked HEMA.

$\phi$ (kGy)	T (K)	$S_t$ (wt%)	$S_{nf}$ (wt%)	$S_f$ (wt%)	$\Delta h_{em}$ (J/g)	$\Delta H_{nf}$ (kcal/mol)	$\Delta H_f$ (kcal/mol)
0	328	54.36 ± 0.30	44.43 ± 0.51	9.93 ± 0.20	282	1.44 ± 0.08	3.01 ± 0.13
	323	55.34 ± 0.33	46.02 ± 0.53	9.32 ± 0.19	285		
	318	56.44 ± 0.58	47.84 ± 0.71	8.61 ± 0.13	287		
	313	57.51 ± 0.53	49.54 ± 0.68	7.97 ± 0.14	290		
	308	58.60 ± 0.43	51.20 ± 0.59	7.40 ± 0.16	292		
160	328	52.42 ± 0.32	43.60 ± 0.50	8.82 ± 0.18	281	1.18 ± 0.05	2.99 ± 0.10
	323	53.32 ± 0.35	45.15 ± 0.52	8.17 ± 0.16	284		
	318	53.85 ± 0.44	46.26 ± 0.58	7.59 ± 0.14	286		
	313	54.80 ± 0.52	47.71 ± 0.66	7.09 ± 0.13	285		
	308	55.60 ± 0.42	49.06 ± 0.56	6.54 ± 0.14	283		
200	328	50.35 ± 0.31	42.46 ± 0.48	7.89 ± 0.17	280	1.10 ± 0.06	2.99 ± 0.12
	323	50.91 ± 0.36	43.52 ± 0.50	7.38 ± 0.13	281		
	318	51.72 ± 0.45	44.90 ± 0.57	6.82 ± 0.11	283		
	313	52.38 ± 0.41	46.02 ± 0.53	6.36 ± 0.11	282		
	308	53.20 ± 0.47	47.33 ± 0.59	5.88 ± 0.12	280		
300	328	47.42 ± 0.35	40.91 ± 0.47	6.51 ± 0.12	279	1.01 ± 0.06	2.98 ± 0.12
	323	48.04 ± 0.42	42.02 ± 0.53	6.03 ± 0.11	282		
	318	48.81 ± 0.37	43.23 ± 0.49	5.58 ± 0.12	283		
	313	49.35 ± 0.39	44.11 ± 0.50	5.24 ± 0.11	283		
	308	50.10 ± 0.53	45.27 ± 0.62	4.83 ± 0.08	280		
400	328	45.77 ± 0.23	36.14 ± 0.41	9.64 ± 0.17	274	1.11 ± 0.05	1.79 ± 0.07
	323	46.44 ± 0.25	37.20 ± 0.42	9.24 ± 0.17	276		
	318	47.09 ± 0.14	38.28 ± 0.30	8.81 ± 0.16	277		
	313	47.70 ± 0.38	39.23 ± 0.54	8.48 ± 0.15	276		
	308	48.45 ± 0.31	40.39 ± 0.46	8.06 ± 0.14	273		

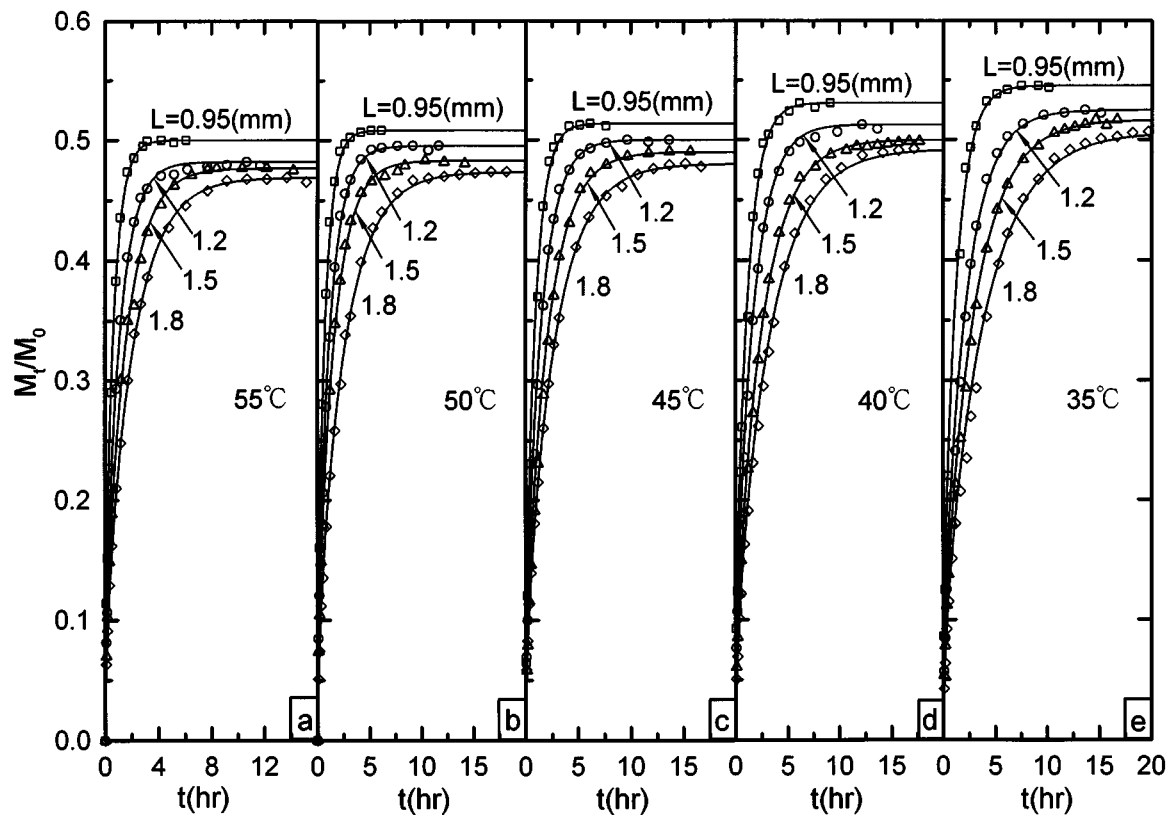


Fig. 5. Water sorption in crosslinked HEMA of different thicknesses: (a)  $T = 55^{\circ}\text{C}$ , (b)  $T = 50^{\circ}\text{C}$ , (c)  $T = 45^{\circ}\text{C}$ , (d)  $T = 40^{\circ}\text{C}$  and (e)  $T = 35^{\circ}\text{C}$ .

diffusion coefficient is almost the same for both sets of specimens, but the velocity for the aged specimen is greater than that for the unaged specimen. The reason why the aged specimen has a higher velocity is not clear at this moment.

The equilibrium-swelling ratio,  $S$ , of water in crosslinked HEMA of different thickness is tabulated in Table 7. For a given temperature, the value of  $S$  decreases with increasing thickness. It is also found that the value of  $S$  decreases with increasing temperature for a given thickness. The line of equilibrium-swelling ratio versus temperature satisfies the van't Hoff plot; and the heats of mixing for various thicknesses are obtained and listed in Table 8. The transport process is exothermic. As can be seen from Table 8, the heat of mixing is almost constant for the thickness in the range of 0.95 mm and 1.8 mm.

#### 4. SUMMARY AND CONCLUSIONS

The water transport in crosslinked HEMA irradiated by  $\gamma$ -ray in vacuum was investigated. The sorption data of water transport in crosslinked HEMA subjected to various  $\gamma$ -ray dosages were in excellent agreement with Harmon's model that accounts for Case I, Case II, and anomalous transport. The diffusion coefficient for Case I and velocity for Case II satisfied the Arrhenius equation for all dosages. The transport process was exothermic and the equilibrium-swelling ratio satisfied the van't Hoff plot. The activation energy for

Case II transport decreased with increasing dosage from 0 to 468 kGy, but that for Case I transport was almost independent of dosage. The heat of mixing was

Table 7. The Diffusion Coefficient  $D$  for Case I, Velocity  $v$  for Case II and Equilibrium-Swelling Ratio  $S$  in Water / Crosslinked HEMA of Different Thicknesses  $L$ .

T (K)	L (mm)	$D \times 10^7$ (cm <sup>2</sup> /sec)	$v \times 10^6$ (cm/sec)	S (wt%)
328	0.95	3.00	2.88	$50.00 \pm 0.23$
	1.20	3.06	2.95	$48.19 \pm 0.27$
	1.50	3.12	3.02	$47.66 \pm 0.27$
	1.80	3.20	3.08	$46.88 \pm 0.27$
323	0.95	2.60	2.53	$50.82 \pm 0.29$
	1.20	2.65	2.60	$49.53 \pm 0.22$
	1.50	2.73	2.65	$48.3 \pm 0.27$
	1.80	2.78	2.70	$47.35 \pm 0.25$
318	0.95	2.21	2.17	$51.38 \pm 0.23$
	1.20	2.24	2.26	$50.01 \pm 0.34$
	1.50	2.27	2.30	$49.00 \pm 0.22$
	1.80	2.35	2.35	$48.01 \pm 0.22$
313	0.95	1.85	1.90	$53.08 \pm 0.24$
	1.20	1.89	1.95	$51.26 \pm 0.23$
	1.50	1.95	2.00	$50.00 \pm 0.23$
	1.80	2.00	2.05	$49.22 \pm 0.27$
308	0.95	1.55	1.60	$54.51 \pm 0.31$
	1.20	1.59	1.65	$52.46 \pm 0.30$
	1.50	1.63	1.69	$51.65 \pm 0.24$
	1.80	1.67	1.73	$50.63 \pm 0.26$

Table 8. Activation Energies of Case I ( $E_D$ ) and Case II ( $E_v$ )/Transport and the Heat of Mixing ( $\Delta H$ ) With Different Thickness L.

L(mm)	0.95	1.20	1.50	1.80
$E_D$ (kcal/mole)	$6.94 \pm 0.13$	$6.88 \pm 0.09$	$6.83 \pm 0.13$	$6.81 \pm 0.09$
$E_v$ (kcal/mole)	$6.11 \pm 0.09$	$6.06 \pm 0.11$	$6.03 \pm 0.08$	$5.98 \pm 0.09$
$\Delta H$ (kcal/mole)	$0.877 \pm 0.095$	$0.828 \pm 0.060$	$0.798 \pm 0.082$	$0.786 \pm 0.086$

greater for the standard specimens than for the specimens with dosage in the range of 160 kGy and 468 kGy.

The pH value of de-ionized water is lower after immersion of crosslinked HEMA. The water was more acidic for immersion with irradiated crosslinked HEMA specimen than for immersion with standard specimen. Acidity of water was increased with the increase of weight loss of specimen. The cutoff wavelength was increased with increasing dosage, but the trend of transmittance was opposite.

For a given dosage, the glass transition temperature of crosslinked HEMA before water treatment was greater than that after water saturation procedure. Both freezing and non-freezing water were analyzed using DSC. Both freezing and non-freezing water satisfied the van't Hoff equation. The former and the latter were endothermic and exothermic processes, respectively. The heat of mixing of freezing water was nearly the same for dosage in the range of  $\phi \leq 300$  kGy and was lowered for  $\phi = 400$  kGy. The heat of mixing is greater for the standard specimen than that for the specimen with dosage  $\phi \geq 160$  kGy.

The effect of thickness on the water transport in standard specimen was studied. The activation energies of diffusion coefficient and velocity were nearly constant regardless of thickness. At a given temperature, the equilibrium-swelling ratio was decreased with increasing thickness. The heat of mixing was almost independent of thickness.

#### ACKNOWLEDGMENT

This work was supported by the National Science Council of Taiwan, Republic of China.

#### NOMENCLATURE

C	=	Concentration of solvent at point X.
$C_0$	=	Concentration of solvent at point X = $\pm \ell$ .
$C_{0x}$	=	Concentration of solvent at point X = 0.
D	=	Diffusion coefficient of solvent transport in crosslinked HEMA.
$E_D, E_v$	=	Activation energies of D and v.
HEMA	=	2-hydroxyethyl methacrylate.
I	=	Transmittance of specimen.
J	=	Total flux of solvent.
L	=	Thickness of specimen.
$\ell$	=	Half-thickness of specimen.
$M_0$	=	Initial weight of specimen.
$M_\infty$	=	Equilibrium weight gain.

$M_t$	=	Weight gain at time t.
$M_{\text{freezing water}}$	=	Mass of freezing water.
$M_{\text{polymer}}$	=	Mass of dry polymer.
m	=	Exponent of time.
n	=	Parameter of solution of diffusion equation.
S	=	Equilibrium swelling ratio.
$S_f$	=	Swelling ratio contributed by freezing water.
$S_{nf}$	=	Swelling ratio contributed by non-freezing water.
$S_t$	=	Total swelling ratio at time t.
T	=	Temperature.
t	=	Time.
$T_{g1}$	=	Glass transition temperature of dry specimen.
$T_{g2}$	=	Glass transition temperature of specimen saturated with water.
v	=	Velocity of solvent transport in crosslinked HEMA.
X	=	Position with respect to the center of specimen.
$\Delta H_f$	=	Heat of freezing water mixing with crosslinked HEMA
$\Delta H_{\text{freezing water}}$	=	Total heat produced by the melting of freezing water.
$\Delta H_{nf}$	=	Heat of nonfreezing water mixing with crosslinked HEMA
$\Delta h_{cm}$	=	The effective specific heat of fusion of water.
$\lambda_n, \beta_n$	=	Parameters of solution of diffusion equation.
$\phi$	=	Gamma ray dosage.

#### REFERENCES

1. M. F. Refojo, *Encyclopedia of Polymer Science and Technology*, pp.195-219, Wiley, New York, (1976).
2. O. Wichterle and D. Lim, *Nature*, **185**, 117 (1960).
3. B. D. Ratner and I. F. Miller, *J. Biomed. Mater. Res.*, **7**, 353 (1973).
4. J. Vacik, M. Czakova, J. Exner and J. Kopecek, *Collection Czechoslov Chem. Commun.* **42**, 2786 (1977).
5. M. Tollar, M. Stol and K. Kliment, *J. Biomed. Mater. Res.*, **3**, 305 (1969).
6. S. M. Lazarus, J. N. LaGuerre, H. Kay, S. R. Weinberg and B. S. Levowitz, *J. Biomed. Mater. Res.*, **5**, 129 (1971).
7. D. G. Pedley, P. J. Skelly and B. J. Tighe, *Br. Polym. J.*, **12**, 99 (1980).
8. J. R. Larke and B. J. Tighe (to National Research Development Corporation), *British Patent*, **1**, 501 (1975).
9. J. J. Janacek, *Macromol. Sci. Rev. Macromol. Chem.*, **9**, 1 (1973).
10. M. F. Refojo, *J. Polym. Sci. A-1*, **5**, 3103 (1967).
11. I. Klotz and J. Franzen, *J. Amer. Chem. Soc.*, **84**, 3461 (1962).

12. H. B. Lee, M. S. John and J. D. Andrade, *J. Colloid and Interface Sci.*, **51**, 225 (1975).
13. Y. K. Sung, D. E. Gregonis, M. S. John and J. D. Andrade, *J. Appl. Polym. Sci.*, **26**, 3719 (1981).
14. G. Smyth, F. X. Quinn and V. J. McBrierty, *Macromolecules*, **21**, 3198 (1988).
15. K. Pathamanathan and G. P. Johari, *J. Polym. Sci.: Part B: Polym. Phys.*, **28**, 675 (1990).
16. R. Jeyanthi and K. P. Rao, *J. Appl. Polym. Sci.*, **43**, 2333 (1991).
17. H. Yasuda, C. E. Lamaze and A. Peterlin, *J. Polym. Sci.: A-2*, **9**, 1117 (1971).
18. N. A. Peppas and N. M. Franson, *J. Polym. Sci.: Part B: Polym. Phys. Edn.*, **21**, 983 (1983).
19. N. M. Franson and N. A. Peppas, *J. Appl. Polym. Sci.*, **28**, 1299 (1983).
20. T. Alfrey, E. F. Gurnee and W. G. Lloyd, *J. Polym. Sci.: C*, **12**, 249 (1966).
21. J. Crank, *The Mathematics of Diffusion*, 2nd Ed., Clarendon Press, Oxford, England (1975).
22. N. L. Thomas and A. H. Windle, *Polymer*, **23**, 529 (1982).
23. C. Y. Hui, K. C. Wu, R. C. Lasky and E. J. Kramer, *J. Appl. Phys.*, **61**, 5129 (1987).
24. S. Govindjee and J. C. Simo, *J. Mech. Phys Solids*, **41**, 863 (1993).
25. W. R. Vieth, J. M. Howell, and J. H. Hsieh, *J. Membr. Sci.*, **1**, 177 (1976).
26. K. I. Okamoto, N. Tanihara, H. Watanabe, K. Tanaka, H. Kita, A. Nakamura, Y. Kusuki and K. Nakagawa, *J. Polym. Sci.: Part B: Polym. Phys.*, **30**, 1223 (1992).
27. K. Toi, T. Ito, T. Shirakawa, and I. Ikemoto, *J. Polym. Sci.: Part B: Polym. Phys.*, **30**, 549 (1992).
28. T. T. Wang, T. K. Kwei and H. L. Frisch, *J. Polym. Sci.: A-2*, **7**, 2019 (1969).
29. T. K. Kwei, T. T. Wang and H. M. Zupko, *Macromolecules*, **5**, 645 (1972).
30. T. K. Kwei and H. M. Zupko, *J. Polym. Sci.: A-2*, **7**, 876 (1969).
31. T. T. Wang and T. K. Kwei, *Macromolecules*, **6**, 919 (1973).
32. H. L. Frisch, T. T. Wang and T. K. Kwei, *J. Polym. Sci.: A-2*, **7**, 8 (1969).
33. J. P. Harmon, S. Lee and J. C. M. Li, *J. Polym. Sci.: Part A: Polym. Chem. Edn.*, **25**, 3215 (1987).
34. J. P. Harmon, S. Lee and J. C. M. Li, *Polymer*, **29**, 1221 (1988).
35. P. P. Wang, S. Lee and J. P. Harmon, *J. Polym. Sci.: Part B: Polym. Phys.*, **32**, 1217 (1994).
36. T. Wu, S. Lee and W. C. Chen, *Macromolecules*, **28**, 5751 (1995).
37. H. Ouyang and S. Lee, *J. Mater. Res.*, **12**, 2794 (1997).
38. H. Ouyang, C. C. Chen, S. Lee and H. J. Yang, *Polym. Sci.: Part B: Polym. Phys.*, **36**, 163 (1998).
39. M. F. Refojo and H. Yasuda, *J. Appl. Polym. Sci.*, **9**, 2425 (1965).
40. P. H. Corkhill, A. M. Jolly, C. O. Ng and B. J. Tighe, *Polymer*, **28**, 1758 (1987).
41. T. C. Warren and W. Prins, *Macromolecules*, **5**, 506 (1972).
42. D. G. Pedley and B. J. Tighe, *Br. Polym. J.*, **11**, 130 (1979).
43. M. A. Frommer and D. Lancet, *J. Appl. Polym. Sci.*, **16**, 1295 (1972).
44. L. A. Wall and R. E. Florin, *J. Appl. Polym. Sci.*, **2**, 251 (1959).
45. C. H. Bamford, A. D. Jenkins, M. C. R. Symons and M. G. Townsend, *J. Polym. Sci.*, **34**, 181 (1959).
46. M. Froix and R. A. Nelson, *Macromolecules*, **8**, 726 (1975).
47. T. Hatakeyama, A. Yamauchi and H. Hatakeyama, *Eur. Polym. J.*, **20**, 61 (1984).
48. S. Krishnamurthy, D. McIntyre, E. R. Santee and C. R. Wilson, *J. Polym. Sci.: B: Polym. Phys. Edn.*, **11**, 427 (1973).
49. M. B. Ahmad, J. P. O'Mahony, M. B. Huglin, T. P. Davis and A. G. Ricciardone, *J. Appl. Polym. Sci.*, **56**, 397 (1995).
50. J. Pouchly, J. Biroš and S. Benes, *Makromol. Chem.*, **180**, 745 (1979).
51. F. X. Quinn, E. Kampff, G. Smyth and V. J. McBrierty, *Macromolecules*, **21**, 3191 (1988).